Journal of Alloys and Compounds 511 (2012) 14–21

Contents lists available at SciVerse ScienceDirect

Journal of Alloys and Compounds

journal homepage: www.elsevier.com/locate/jallcom

Reliability of anodic vacuum arc in depositing thermoelectric alloy thin films

S.K. Mukherjee*, P.K. Barhai

Department of Applied Physics, Birla Institute of Technology Mesra, Ranchi 835215, Jharkhand, India

ARTICLE INFO

Article history:
Received 7 January 2011
Received in revised form 30 June 2011
Accepted 4 September 2011
Available online 10 September 2011

Keywords:
Anodic vacuum arc
ICP-OES
Thin films
Constantan
Chromel
Alumel

ABSTRACT

Inductively coupled plasma optical emission spectrometry (ICP-OES) was applied for the analysis of major and minor elements of thermoelectric alloys (Constantan, Chromel and Alumel) and their thin films deposited using anodic vacuum arc (AVA) plasma deposition technique. Digestion of samples was done in aqua regia. The minor and trace elements were determined without matrix separation. The precision for all the constituents was <3%. The changes in the composition of these alloy films were studied as a function of number of deposition cycles and also with various positions of the samples on the substrate holder. Due to the difference in the evaporation rates of the alloy constituents and the interaction of Ni with the refractory basket, the AVA deposited films showed varying compositions in the initial cycles of deposition. However, a good agreement was obtained among the samples deposited on various positions of the substrate holder, suggesting a uniform plasma flux in the system. Films deposited using Constantan wires were much enriched with Cu. By depositing bilayers of Cu and Ni, followed by post annealing, we were able to produce films in which the Cu and Ni concentrations were similar to that of Constantan. A deviation of ~15% was observed among 10 Cu films of thickness ~300 nm deposited using this technique. AVA deposited films of Chromel and Alumel having Ni (≥90%) could be developed without much alteration in their composition.

© 2011 Elsevier B.V. All rights reserved.

1. Introduction

There are many types of thermocouples but only a small number of them have been standardized to the point of having distinct calibration tables, color codes and assigned letter designations that are recognized worldwide. The ASTM standard E230 provides all the specifications for most of the common industrial grades, including letter designations, color codes, suggested temperature limits and the complete voltage versus temperature tables [1]. Common commercially available thermocouples are specified by ISA (Instrument Society of America) types. Type J, T, E, and K are base-metal thermocouples [1]. All these commercial thermocouples are alloy-based. Normally the thermoelectric power (TEP) of metals can be altered by adding elements or impurities. Commonly desired characteristics of these alloying elements are: good solubility, possible improvement of mechanical properties, resistance to corrosion, and stabilization of the thermoelectric power [2]. The TEP has to be easily reproduced and should be least sensitive to slight variations in the chemical content. Within Ni–Cr alloys the Seebeck coefficient varies from negative values typical of pure nickel (TEP = $-17.7\,\mu V/{}^{\circ}C$ at $0\,{}^{\circ}C$) to positive values typical of pure chromium (TEP = $+20.3\,\mu V/{}^{\circ}C$ at $0\,{}^{\circ}C$). One such composition is selected which corresponds to an almost flat maximum in the thermoelectric output curve for the nominal percentages of alloying elements [3]. This composition is termed as Chromel. Chromel contains 89–90% Ni, 9–9.5% Cr by weight with Si, Fe, Mn, C, Co and/or Nb as trace materials (below 1%) [2]. On the other hand, a Ni–Al based alloy (Alumel) has been developed with the requirement of matching with Chromel according to a linear EMF–temperature relation. Alumel contains 95–96% Ni, 1–1.5% Si, 1–2.3% Al, 1.6–3.2% Mn and Co, Fe, Cu and Pb as trace materials [2]. “Chromel” and “Alumel” are the trademarks of Hoskins Manufacturing Company. This company was the sole manufacturer of Chromel–Alumel thermocouples (Type K) in USA until the mid-1940. Likewise, one more alloy has been chosen for commercial thermocouples, named Constantan. The word Constantan denotes a family of Cu–Ni alloys with 45–60% Cu. The composition intended to be used for thermocouples (Type T, Type E and Type J) should contain 55–57% Cu and 43–45% Ni with some but thermoelectrically significant amounts of Fe and/or Mn [2]. Constantan is the trademark of Wilbur B. Driver Company.

It is well known that the properties of a thin film may be quite different from those of its bulk, particularly if the film thickness is very small. These anomalous properties are due to the peculiar structure and varying composition of the film, which in turn, is governed by the processes which occur during film formation [4,5]. Film composition plays a very significant role in deciding the transport parameters such as, resistivity, temperature coefficient of resistance, thermoelectric power, etc., in a thin film. Often

* Corresponding author. Tel.: +91 943 1363464; fax: +91 651 2275401.
E-mail address: sanat_aphy@yahoo.co.in (S.K. Mukherjee).

0925-8388/$ – see front matter © 2011 Elsevier B.V. All rights reserved.
doi:10.1016/j.jallcom.2011.09.013

the composition of a film varies during deposition whatsoever the technique may be. This is primarily due to the processes involved in their deposition. In conventional evaporation techniques, it is the vapor pressure of the constituent elements of an alloy which decides the final stoichiometry of an alloy thin film while in sputtering, it is the sputter yield of the constituents which decides the final composition [4,5].

Anodic vacuum arc (AVA) with cathodes operating in the spot mode and hot evaporating anodes providing the evaporating material offer an energetic tool for producing thin films. This technique has various advantages over other deposition techniques. AVA is a source of pure metal vapor plasma free from macroparticles that offers various advantages like, high deposition rates, low thermal load on the substrate, and high degree of ionization with energetic ions [6–8] over other deposition techniques. Flux ionization can be varied significantly from 1% to 30% while ion energies range from 2 to 150 eV offering a better control over the deposition process [9]. Deposition rate up to 40 nm/s is achievable with input power in the range of 400–900 W that is much higher than those obtainable by using other physical vapor deposition (PVD) processes. For example, in sputter deposition even with much higher power inputs the sputter rates are quite low [10]. The high deposition rate (5–40 nm/s) of AVA coupled with macroparticle free stream of highly ionized energetic particles makes it industrially viable.

In this paper the reliability of anodic vacuum arc plasma deposition technique in developing thermoelectric alloy thin films was examined in terms of a comparative compositional analysis using inductively coupled plasma-optical emission spectrometry (ICP-OES) between the deposited alloy films and their corresponding bulk metal alloys (Constantan, Chromel and Alumel). The thermoelectric properties of the resulting films were published elsewhere [11] and hence, not included in the present manuscript.

2. Experimental details

Before investigating the reliability of AVA in depositing thermoelectric alloy thin films, it should be noted that these thermoelectric alloys are chemically inhomogeneous (composition changes from point to point). Inhomogeneities in a thermoelectric wire are caused by mechanical factors primarily leading to short ranged ordering along the length of the thermoelements [2,3]. As such, compositions of macroscopically bigger areas need to be determined to specify the overall composition of these thermoelectric alloys. Among the various chemical methods used for overall compositional analysis, inductively coupled plasma-optical emission spectrometry is the most precise technique [12]. ICP-OES is a multi-element technique that allows the determination of major, minor and trace elements in complex samples [12–14]. It is also known as inductively coupled plasma-atomic emission spectrometry. It involves electromagnetic radiation (light) that is absorbed by and/or emitted from atoms of a sample. In ICP-OES, the sample is usually transported into the instrument as a stream of liquid sample. Inside the instrument, the liquid is converted into an aerosol through a process known as *nebulization*. The sample aerosol is then transported to a small chamber where it is subjected to temperatures high enough to cause desolvation, vaporization, atomization and finally excitation and/or ionization. Fig. 1 shows a schematic representation of the process involved in compositional analysis using ICP-OES. Ar-supported inductively coupled plasma is used as atomization/excitation source to dissociate sample molecules into free atoms. Once the atoms or ions are in their excited states, they can decay to lower states through their characteristic thermal or radiative (emission) transitions which are collected by a device that sorts the radiation by wavelength. The radiation is detected and turned into electronic signals. The intensity of the radiations emitted at specific wavelengths is thus measured and used to determine the concentrations of the element of interest.

The ICP-OES technique is applicable for the determination of a large number of elements. A major advantage of ICP-OES is that many elements can be determined easily in the same analytical run. This multi-element capability arises from the fact that all of the emission signals needed to obtain qualitative and quantitative information is emitted from the plasma at the same time. The precision and accuracy of the ICP-OES analyses are very high for most trace elemental analyses. Precision of analysis is less than ±1% while its accuracy is within ±2% when the concentration is greater than hundred times the detection limit [12]. The detection limit is the lowest concentration at which the analyst can be relatively certain that an element is present in a sample. In ICP-OES, the detection limits for these elements are generally in the μg/L (parts per billion) range. Analytical qualities such as, relatively low detection limits, capacity for simultaneous, rapid and precise determinations over wide

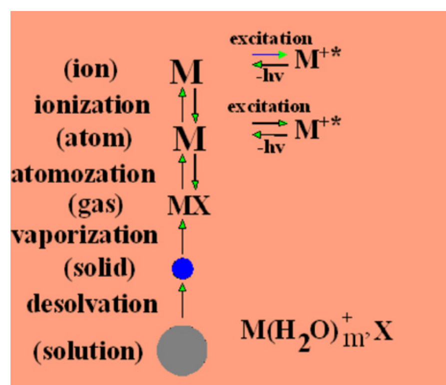

Fig. 1. Schematic representation of the process involved in compositional analysis using ICP-OES.

concentration ranges have made ICP-OES the choice for multi-elemental analysis and preferred over other techniques such as atomic absorption spectrometry, flame atomic absorption spectrometry, instrumental neutron activation analysis and X-ray fluorescence. Details of the experimentation involved in ICP-OES measurements for the present work are described below.

2.1. Instrumentation

All the measurements were performed with a PerkinElmer model Optima 2100DV inductively coupled plasma optical emission spectrometer equipped with a dual echelle type monochromator with an echelle grating of 79 lines/mm at a blaze angle of 63.8° and a 40 MHz free-running solid state radio frequency (RF) generator with an output power range of 750–1500 W. A Scott type double-pass spray chamber and a HF resistant Gem-Cone cross-flow pneumatic type nebulizer were used throughout. A peristaltic pump was used to feed the nebulizer system with sample solution. A solid-state two-dimensional CCD detector of 25,600 pixels was used for detecting the spectra. The ICP-OES instrument employed in this study used an axially viewed configuration that generally provides better detection limits than radially viewed plasmas [15]. This configuration increases the amount of radiation energy that reaches the entrance slit of the monochromator. Plasma torch alignment was performed by using Mn II emission line at 257.610. The determination of element concentrations was performed with default parameters optimized to guarantee maximum analyte signal, low signal-to-background ratio (SBR), enable proper correlation with calibration standards, and to obtain plasma stability. The instrumental operating parameters are summarized in Table 1. The conditions were optimized for the Ni II emission line (232.604 nm) which is the major constituent of all the alloys under test. These parameters were set in order to attain robust plasma conditions [13]. The term "robustness" is used to describe the excitation and atomization conditions in the inductively coupled plasma. A robust plasma can be obtained when using a low nebulization Ar flow rate, an elevated RF power, and a central injector with an internal diameter equal to or larger than 2.0 mm. Silva et al. [13] showed that the best detection limits were obtained using ICP-OES in axial configuration under robust conditions. Because of the complexity of the spectra of the analyte, a careful selection was conducted to avoid spectral interferences. All the analytical emission line wavelengths employed for measurements are listed in Table 2. Spectrum scans were performed in the vicinity (±0.009 nm) of each chosen wavelength. Off-peak background correction was carried out at both sides of the analyte peak.

Table 1
Operating conditions of the inductively coupled plasma-optical emission spectrometer.

RF power	1300 W
Nebulizer argon flow	0.80 l/min
Auxiliary argon flow	0.20 l/min
Plasma argon flow	1.5 l/min
Shear gas flow	(18–20) l/min
Sample flow	1.5 ml/min
Spectral band pass	0.009 nm at 200 nm, 0.027 nm at 700 nm
Spray chamber	Scott-type
Injector tube diameter	2.0 mm
Source equilibration time	15 s
Viewing height	10 mm
Read delay	30 s
Rinse delay	20 s
Flush time	5 s
Number of replicates	3

Table 2
ICP emission lines used for measurement.

Sample	Element	Emission line (nm)
Constantan	Ni	232.604
	Cu	327.393
	Fe	238.204
	Mn	257.610
Chromel	Ni	232.604
	Cr	267.716
	Fe	238.204
	Mn	257.610
	Co	228.616
	Nb	309.418
Alumel	Ni	232.604
	Al	396.153
	Mn	257.610
	Co	228.616
	Fe	238.204
	Cu	327.393
	Pb	220.353

2.2. Reagents

All reagents employed were of analytical grade. All solutions were prepared with ultra-pure deionized water of resistivity 18 MΩ-cm obtained from a Milli-Q purification device (Millipore Co., Milford, MA, USA). Reagents used for the sample digestion were 65% (v/v) HNO_3 (Merck, Darmstadt, Germany) and 37% (v/v) HCl (Merch, Darmstadt, Germany). Aqua regia was prepared by mixing HNO_3 and HCl in the ratio 1:3. Multi-element standard stock solution for ICP measurements containing 100 mg/L of the elements under investigation namely, Ni, Cu, Cr, Al, Mn, Co, Fe and Pb (Merck, Darmstadt, Germany) was used for calibration.

2.3. Calibration

All the concentration measurements were carried out using a four-point calibration. Multi-element calibration solutions containing the above mentioned elements in the concentration range 0.01–10 mg/L were prepared by serial dilution of the ICP stock solution in order to obtain the aqueous and matrix matching calibration curves constructed with 0.01, 0.1, 1 and 10 mg/L of elements. The optimization for each element was performed by taking the analytical emission lines chosen for measurement (see Table 2).

2.4. Sample preparation

One of the most important requirements of a spectrochemical analysis is the sample preparation procedure, which must be simple and able to transform the sample to a form compatible with the introduction system and atomizer. Both thin film and wire samples of Constantan, Chromel and Alumel were digested in 10 ml solution of aqua regia and were subsequently diluted using Milli-Q water to 1 L. In case of wire samples, the amount of material digested was estimated by weighing them in a high resolution (least count = 1 μg) weighing balance (Mettler Toledo, model: MX5). Thin film samples on microscopic glass slides of dimensions 24 mm × 24 mm × 0.1 mm were weighed prior to their digestion. After weighing these deposited glass slides were dipped in 10 ml aqua regia. After complete dissolution of the films, the glass slides were taken out, rinsed in Milli-Q water, dried and weighed again. The difference between these two weights gives the amount of thin film material utilized in digestion.

3. Results and discussion

3.1. Compositional analysis using ICP-OES

To investigate the reliability of AVA in depositing alloy thin films, wires of Constantan, Chromel and Alumel were used as a source material. The compositions of these alloy wires were determined using ICP-OES and are listed in Table 3.

3.1.1. Variation of film composition with the number of deposition cycles

A small quantity (300 mg) of these alloy wires were twisted into a spherical mesh and placed within the refractory basket made up of tungsten in the present case. It was also ascertained that the entire source gets consumed in each deposition. On starting deposition with a new tungsten basket, it was observed that the composition of the alloy films deposited using their respective wires vary in first few deposition cycles. Figs. 2–4 show the variation in the percentage of constituent elements of the films deposited using Constantan, Chromel and Alumel wires with respect to the number of deposition cycles using the same tungsten basket. The changes in the percentage of constituent elements are more pronounced in the films deposited using Constantan wires. It has been observed that the Cu percentage in the film deposited first (using a new tungsten basket) is 86.3%, which is much higher than its content in the source material (54%). Likewise, the Ni content in the film deposited first was very less (∼12%) instead of 44% in the bulk Constantan wire (see Fig. 2a and b). The vapor pressure at the anode operating temperature of Cu was considerably higher than that of Ni. At the anode operating temperature, the vapor pressure of Cu lies between 10^3 and 10^4 Pa while that of Ni is between 10^2 and 10^3 Pa [16]. Hence, the evaporation rate of Cu is higher. Moreover, Ni possesses a strong tendency to form alloy with refractory metals while Cu has practically no interaction with refractory materials [5]. Some of the Ni melts react with the material of the basket (W). Thus, Ni percentage in the source composition decreases, which in turn, reduces its content in the resulting film. Due to the variation in vapor pressure of the constituent elements, these films also possess a concentration gradient along the film thickness. However, upon annealing at 300 °C for 5 h Ni diffuses into Cu homogenizing the film composition. These results were confirmed using secondary ion mass spectroscopy (SIMS) depth profiling and were published elsewhere [11].

In addition, Fig. 2 also reveals that Cu percentage in the films decreases gradually till the fifth deposition after which it becomes almost constant. The percentage at which Cu stabilizes is ∼66%, which is still higher than that of the source material (54%). Likewise, the Ni content in the films gradually increases with the number of depositions using the same tungsten basket. Ni percentage finally stabilizes after the fifth deposition to ∼33%, which is lower than that of the Constantan wire (44%). As soon as the arc initiates the source which was kept in the form of a spherical mesh within the basket forms a small spherical drop of liquid that settles at the bottom of the basket. From the liquid drop the source material advances to the inner walls of the chamber in the form of plasma with a conical flux distribution. Ni within the source material reacts with the material of the basket in two competing ways: first, it wets the portion of the basket where it settled as a liquid drop. Second, when it advances in the form of plasma, it wets the remaining portion of the basket. However, as the deposition process is very fast, it ends within few seconds. In such a short period Ni cannot saturate the basket completely. With every deposition cycle, some amount of Ni

Table 3
Chemical composition (in wt.%) of alloy wires determined using ICP-OES. These values are an average of 10 different samples digested using 10 different pieces of individual wires.

Alloy	Ni	Cu	Cr	Al	Fe	Mn	Pb	Co	Rest[a]
Constantan	43.87 ± 0.82	54.87 ± 0.74	–	–	0.36 ± 0.18	0.79 ± 0.07	–	–	0.10 ± 0.01
Chromel	89.33 ± 0.43	0.24 ± 0.13	9.59 ± 0.36	–	0.57 ± 0.28	–	0.22 ± 0.10	0.02 ± 0.01	0.23 ± 0.08
Alumel	94.83 ± 1.06	0.32 ± 0.22	–	0.65 ± 0.28	0.56 ± 0.17	1.88 ± 0.33	0.24 ± 0.13	0.03 ± 0.01	1.73 ± 0.49

[a] The percentage of chemical contents of the respective alloy wires shown in this column remain undetected.

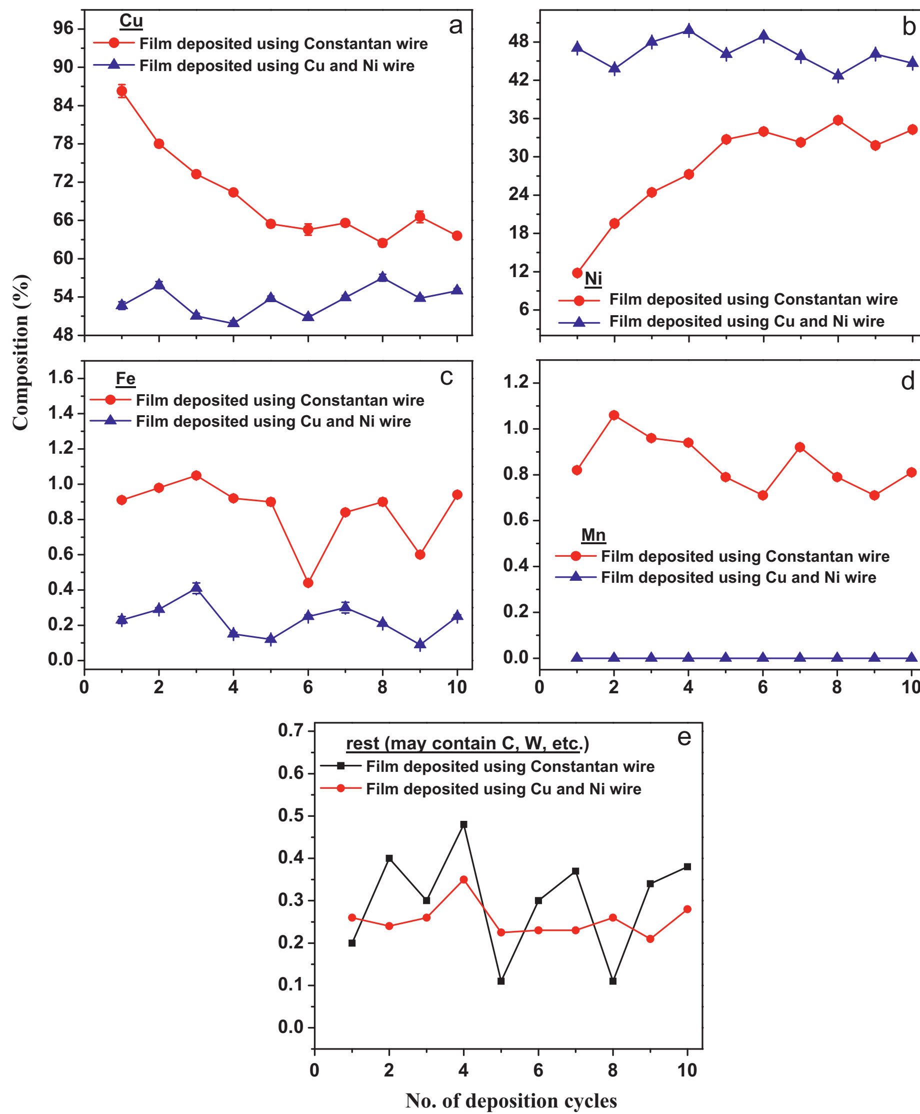

Fig. 2. Variation in the weight percentage of (a) Cu, (b) Ni, (c) Fe, (d) Mn and (e) other impurities (rest) with the number of deposition cycles (starting with a new basket) in the AVA deposited films using Constantan wires and using individual Cu and Ni wires.

from the liquid drop gets absorbed into the basket but the tendency to absorb Ni from the liquid drop decreases as the portion saturates gradually. This is the reason why the Ni percentage is least in the films deposited first and increases gradually in the films till the fifth cycle of deposition. After the fifth cycle of deposition, the portion where the liquid drop settles becomes almost saturated with Ni. As a result, the loss of Ni percentage due to wetting a portion of the basket reduces to almost a negligible amount. However, its loss due

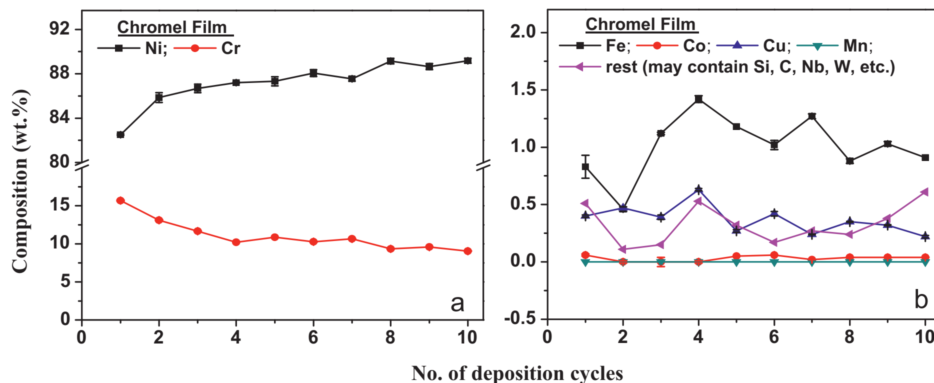

Fig. 3. Variation in the weight percentage of (a) primary elements (Ni and Cr) and (b) known trace elements (Fe, Co, Cu, Mn and other impurities (rest)) with the number of deposition cycles (starting with a new basket) in the AVA deposited films using Chromel wires.

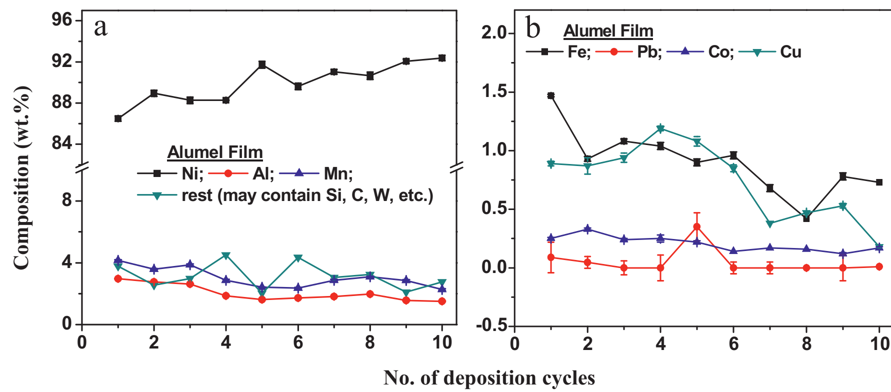

Fig. 4. Variation in the weight percentage of (a) primary elements (Ni, Al, Mn) and rest elements and (b) trace elements (Fe, Pb, Co and Cu) with the number of deposition cycles (starting with a new basket) in the AVA deposited films using Alumel wires.

to the interaction of the plasma with the material (W) of the basket still remains. This may be the reason why Ni stabilizes at a lower value. On the other hand, Cu has practically no interaction with refractory baskets. But as the Ni content in the source decreases, the source becomes relatively more Cu-rich. This enhanced Cu content in the source is reflected in the resulting films (see Fig. 2a and b).

It is noteworthy that the film compositions can be made closer to their respective bulks either by [5]:

(a) changing the source composition,
(b) by limiting the charge used for deposition at a time,
(c) by successively feeding an alloy wire during evaporation, or
(d) by using crucibles made up of non-reactive refractory oxides such as Al_2O_3 and ZrO_2.

An attempt has been made to deposit stoichiometric Constantan films using AVA by doing bilayer deposition of elemental Cu and Ni films. Ni forms solid solution with Cu and has 100% solubility in Cu matrix. The final alloy composition is decided by the individual layer thickness of Cu and Ni. Fig. 2(a and b) shows that the percentage of Cu and Ni remain fairly uniform with number of depositions. The deviation in composition is due to the variation in thickness of Cu and Ni layers. Individual layer thicknesses are maintained by actuating the substrate shutter. As AVA offers a very fast deposition rate, it is very hard to maintain exact film thickness in every deposition. A deviation of ~15% is observed in 10 depositions of Cu films of thickness ~300 nm. Trace elements (Fe and Mn) do not show any definite trend of change with the deposition cycles either in case of films deposited using Constantan wires or in case of bilayer deposition of films using separate Cu and Ni wires (see Fig. 2c and d). However, in bilayer deposition of films using separate Cu and Ni wires, these trace elements are less (Fe varies within 0.05–0.40% while Mn is absent). It is because these depositions were carried out using pure Cu (99.98%) and pure Ni (99.98%)

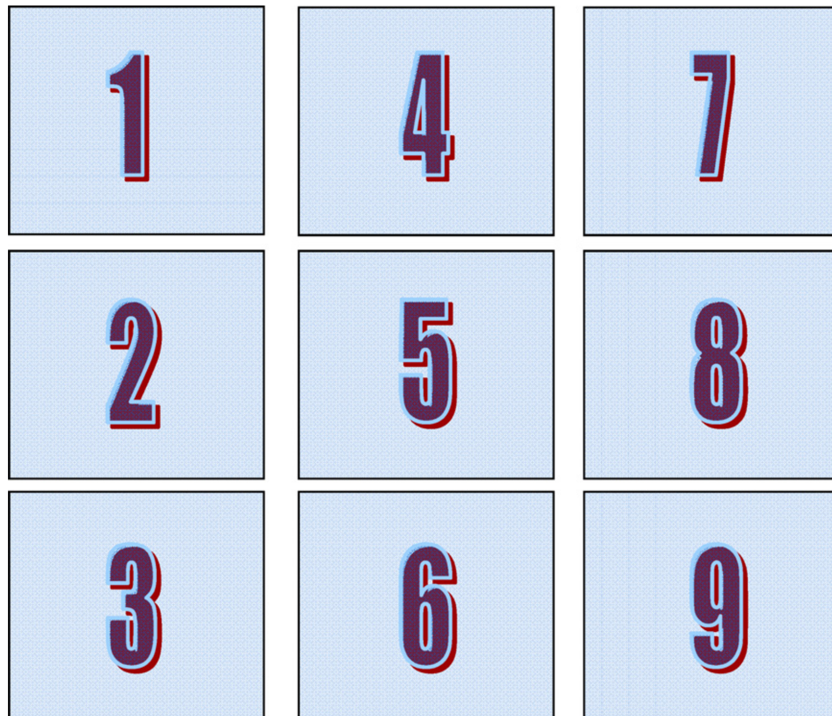

Fig. 5. Schematic representation of the samples arranged in the substrate holder for the investigation of the distribution of film composition along the various sections of the substrate holder.

wires which contain trace of Fe as one of the impurities while they do not contain Mn at all. Apart from the primary constituents (Cu and Ni) and the trace elements (Fe and Mn) some other impurities (<0.5%) are also present in the deposited films (expressed as rest in Fig. 2e). This may include C which may get incorporated into the film due to the graphite cathode or W due to the tungsten basket or some other impurities. C being a nonmetal cannot be detected using ICP-OES and W was not checked because its standard was not available in the laboratory for calibration.

Fig. 3 shows that the Ni content in the films deposited using Chromel wires increases with the number of deposition cycles while the Cr content decreases. However, this variation in Ni and Cr content is relatively less pronounced than that in films deposited using Constantan wires. Moreover, this variation is distinct only in the first few deposition cycles after which the film composition becomes fairly constant. The Ni and Cr content of the film deposited in the first deposition cycle (with a new tungsten basket) is 82.5% and 15.7%, respectively. After three depositions, the Ni and Cr content in the resulting films stabilizes at ~88.5% and ~11%, respectively. These values are close to that of bulk Chromel wire (see Table 3). Cr sublimes on heating and has practically no interaction with the refractory basket [17]. But as its content is less in Chromel, the effect is less reflected in the resulting films especially after few initial deposition cycles. Among the known trace elements, Fe, Cu, Co and Mn do not show a definite trend of change with deposition cycles. Fe content in the films is higher (~1.0%) while Cu content is meager (0.6%). Mn and Co content are negligible in the films. The Chromel wire used in deposition contains these trace elements almost in the same proportion. Other known trace elements (Si, Nb) were not identified as the calibration standard for Nb was not available and Si is insoluble in aqua regia which is used as digestive medium in our case. Apart from the primary constituents (Ni and Cr) and the identified trace elements (Fe, Cu, Co, Mn), some other impurities like Si, C, W, Nb, etc., may also present in the deposited films but in negligible amount (<0.6%) (see Fig. 3b).

Fig. 4 shows the variation of alloy constituents with number of deposition cycles in the films deposited using Alumel wires. The Ni content in the film deposited first (using a new tungsten basket) is 86.5%, which increases with the number of deposition cycles. But this change is less than that in films deposited using Constantan and Chromel wires. The change in Ni percentage is relatively less. In first five depositions, Ni content changes ~5% while in the later depositions, the change is ~3%. This is because Ni comprises the major constituent (95%) of the Alumel alloy. Moreover, Al (1–2.3%) and Mn (1–2.3%) which are the other two primary constituents also possess a tendency to react with the tungsten basket. The presence of Si (1–1.5%) which is another primary constituent of Alumel was not confirmed with ICP-OES. After five depositions, Ni, Al and Mn content in the Alumel films stabilize at ~91%, ~2% and ~2.5% respectively. All the trace elements known to be present in Alumel were also present in their resulting films. The abundance of Fe (1.5–0.5%) and Cu (1.2–0.5%) were relatively more than Co and Pb which are negligible. These trace elements do not show a definite trend of change with the number of deposition cycles (see Fig. 4b). Also, about 4% of the composition was left unconfirmed which may contain Si and impurities like C, W, etc. (see Fig. 4a).

3.1.2. Distribution of film composition along various positions of the substrate holder

A further step to check the reliability of AVA in depositing these thermoelectric alloys is to know whether the distribution of composition of the films deposited in one deposition cycle is uniform along the different positions of the substrate holder or not. It can be ascertained in two ways: either by investigating the plasma along different sections of the substrates for detecting as well as estimating various chemical species present in it or by investigating the chemical composition of the films deposited along the various sections of the substrate holder in a single deposition. Plasma diagnosis, either for identifying or for quantifying chemical species or both would be fruitful in slow deposition techniques like sputtering [18]. In fast deposition techniques like AVA, plasma composition changes instantaneously and hence, the simultaneous determination of chemical species present along the various sections of the substrate holder is very difficult. The determination of film composition is relatively simpler and practically more relevant.

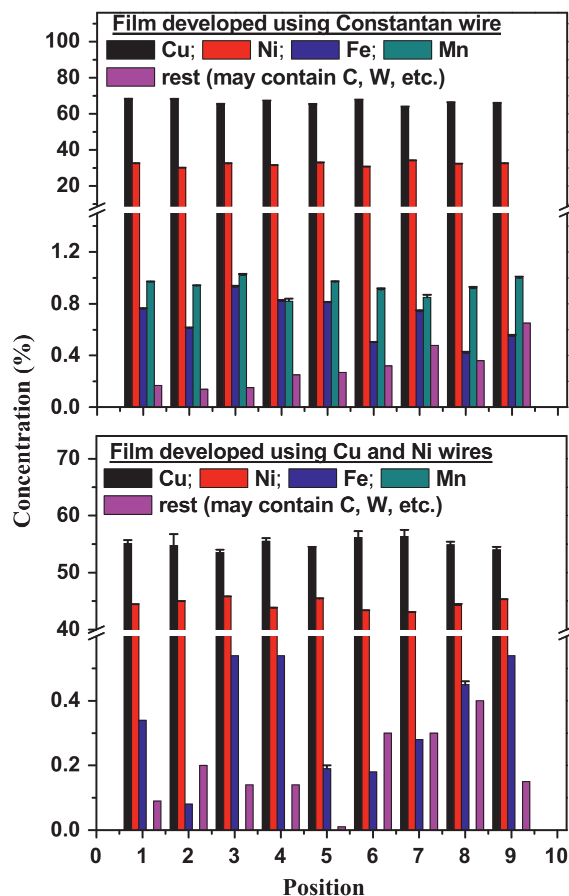

Fig. 6. Distribution of film composition deposited using (a) Constantan wire and (b) Cu and Ni wire along the various sections of the substrate holder.

For the present study, three glass slides of dimension 75 mm × 25 mm × 1.3 mm were sliced into nine equal pieces, cleaned and arranged in a substrate holder of dimension 110 mm × 110 mm. The anode to substrate distance was maintained at 210 mm. Fig. 5 shows the schematic representation of the sample arrangement in the substrate holder for the present study. The compositions of the films deposited on these samples are correlated with the numbers assigned to the various sections of the substrate holder (see Fig. 5). Fig. 6 shows the distribution of alloy components in the films deposited using Constantan wire and by using separate Cu and Ni wires along the various sections of the substrate holder. It has been observed that the film composition remains fairly uniform. However, little inhomogeneity appears along the various sections of the substrate holder. The spread in composition along the various sections of the films deposited using Constantan wires (64–68%) are relatively more than that of films deposited using separate Cu and Ni wires (54–56%). Such a spread of composition in the films may appear due to two possible reasons: first, due to the inherent inhomogeneity in the Constantan wire used for deposition and second, due to the irregularity in the shape

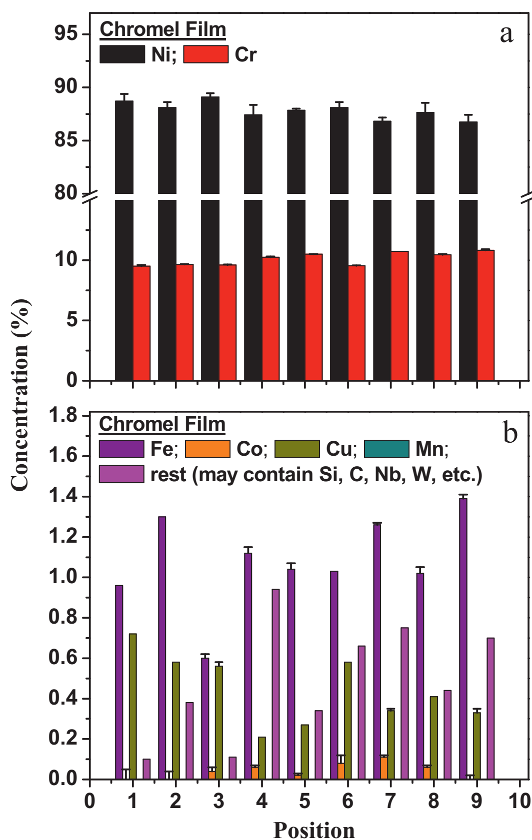

Fig. 7. Distribution of (a) primary constituents and (b) trace elements including the rest (constituents not confirmed) of Chromel alloy in films deposited using Chromel wire along the various sections of the substrate holder.

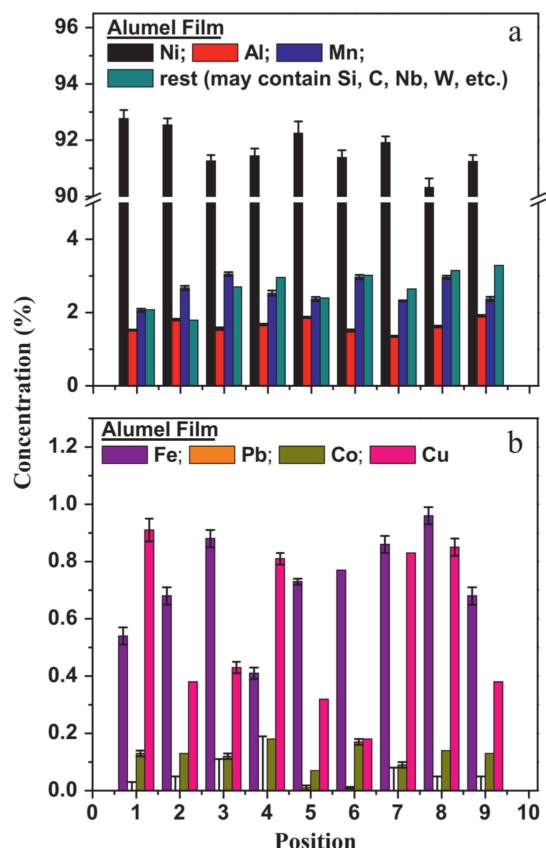

Fig. 8. Distribution of (a) primary constituents including rest (constituents not confirmed) and (b) trace elements of Alumel alloy in films deposited using Alumel wire along the various sections of the substrate holder.

(spherical mesh) of the wire piece in which it is twisted before introducing it into the tungsten basket. However, the inhomogeneity introduced in the resulting films due to the second cause is significant only during the initial stages of film deposition. After the first few seconds of arc initiation the irregular spherical wire mesh melts and settles at the base of the tungsten basket uniformly. The individual Cu and Ni wires do not contain any other alloying element and hence impart less inhomogeneity in the resulting films.

It has also been observed that the impurity content (percentage composition left undetected) in the films slightly increases as one moves from the left section (nos. 1–3) to the right one (nos. 7–9) (see Fig. 6). These impurities may contain C, W, etc. The substrates placed along the right hand section can see the graphite disk of the cathode to some extent in spite of the cathode shutter. As a result there is a possibility that C gets incorporated relatively more into the films deposited along the right section.

Similarly, the films deposited using Chromel and Alumel wires along the various sections of the substrate holder are fairly homogeneous (see Figs. 7 and 8). The slight inhomogeneity that appears along the various sections of the substrate holder may be due to the inherent inhomogeneity of these wires and due to the irregularities in the shape of the spherical mesh. In these films also, the impurity content enhances as one proceeds from the left section to the right one (see Figs. 7b and 8b).

3.2. SIMS depth profile studies

It has been mentioned earlier that an attempt was made to develop more stoichiometric Constantan films by depositing bilayer films of Cu and Ni using elemental Cu and Ni wires. But this technique will work only if Cu and Ni in the bilayers diffuse completely to form Cu–Ni alloy. In order to identify the distribution of Cu and Ni in one such bilayer film and their inter-diffusion upon annealing, SIMS depth profiling has been done. Fig. 9(a) shows the SIMS depth profile of Ni, Cu, O and Si in the as-deposited bilayer film. It can be seen that a small amount of Ni penetrates into the Cu film at the interface. This is due to the energetic deposition which AVA offers. The presence of O and Si in the film is negligible except few small humps of O at the surface, at the interface and near the substrate (Fig. 9a). The hump at the surface is probably due to formation of an oxide layer at the surface, primarily NiO. The hump at the interface is due to the formation of an oxide layer at the surface of the freshly deposited Cu film due to the time lag between Cu and Ni depositions while the hump near the substrate might be due to trapped oxygen between the Cu film and the substrate. However, from the intensities of O it is evident that its presence is negligible.

Fig. 9(b and c) shows the diffusion of Ni of a bilayer film (of Ni and Cu) into the Cu matrix and vice versa by annealing it under vacuum (10^{-3} Pa) at 500 °C for 3 h and 6 h respectively. As Ni diffuses into Cu, O present at the interface disappears. This implies that presence of O at the interface between Ni and Cu film does not affect their inter-diffusion and it finally goes off in the final solid solution. A small amount of O remains at the film surface. The film surface usually possesses enhanced reactivity and reacts with the residual O present in the environment during annealing. Fig. 9(b) shows that even after annealing the bilayer film (shown in Fig. 9a) for 3 h, Ni does not diffuse completely. The surface remains a Ni-rich. However, after annealing for 6 h, complete homogeneity has been achieved.

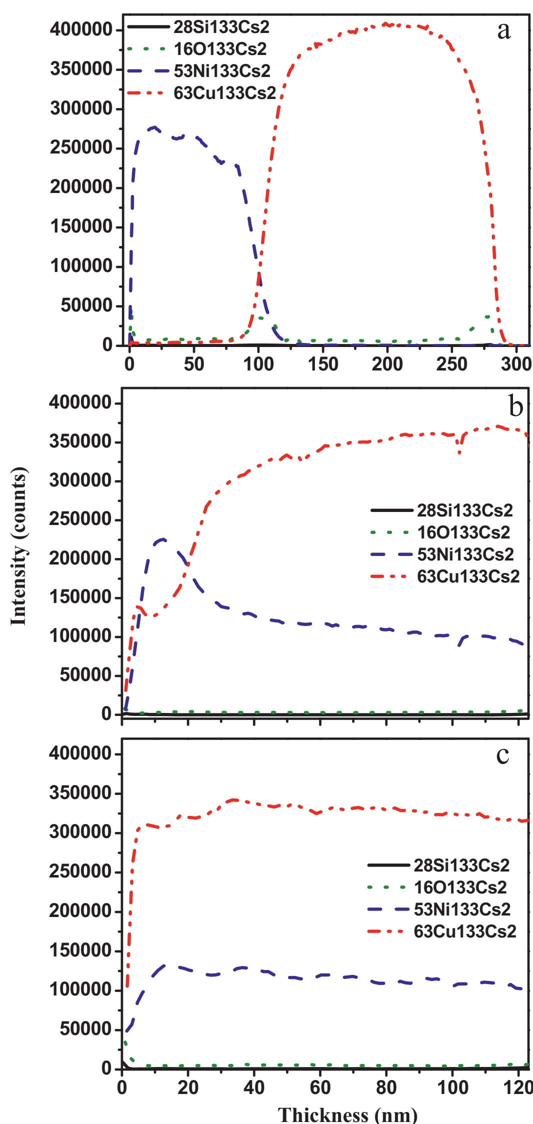

Fig. 9. SIMS depth profiling of AVA deposited Cu and Ni bilayer thin film. (a) as-deposited, (b) annealed at 500 °C for 3 h and (c) annealed at 500 °C for 6 h.

4. Conclusions

A comprehensive analysis has been done on the composition of Constantan, Chromel and Alumel alloys and their anodic vacuum arc deposited films using ICP-OES. On starting deposition with a new tungsten basket, it has been observed that the composition of alloy films deposited using their respective wires vary in first few deposition cycles. The changes in percentage of the constituent elements are more pronounced in films deposited using Constantan wires. Films deposited using Constantan wires show a poor maintenance of stoichiometry. Necessary modifications such as, varying the source composition or more appropriately, co-depositing Cu and Ni, are needed for developing more stoichiometric Constantan films. We succeeded in depositing more stoichiometric Constantan films by doing layered deposition of Cu and Ni, followed by post annealing at 500 °C for 6 h. AVA has been found suitable for depositing Chromel and Alumel films to a fair degree of repeatability. Films deposited using Chromel and Alumel wires show less alteration in their composition. After first few initial cycles, films deposited using Chromel wires show a chemical composition of Ni (∼88.5%) and Cr (∼11%) while that of Alumel is Ni (∼91%), Al (∼2%) and Mn (∼2.5%). The rest comprises of the trace elements.

Acknowledgements

We wish to thank the administration of Birla Institute of Technology, Ranchi for its continued support and financial assistance and Mr. Sanjay Swain and Mr. Ashwini Singh of the Central Instrumental Facility (CIF) at Birla Institute of Technology, Ranchi for their help in ICP-OES measurements. S. K. Mukherjee is also grateful to CSIR, New Delhi, India for the award of Senior Research Fellowship.

References

[1] R.L. Powell, W.J. Hall, C.H. Hyink Jr., L.L. Sparks, G.W. Burns, M.G. Scroger, H.H. Plumb, Thermocouple Reference Tables based on IPTS-68 (NBS Monogram 125), National Bureau of Standards, Washington, DC, 1974.
[2] M. Campari, S. Garribba, Rev. Sci. Instrum. 42 (1971) 644–653.
[3] B. Sundqvist, J. Appl. Phys. 72 (2) (1992) 539–545.
[4] K.L. Chopra, Thin Film Phenomena, Robert E. Krieger, Huntington, 1979.
[5] L.I. Maissel, R. Glang, Handbook of Thin Film Technology, McGraw-Hill, New York, 1970.
[6] H. Ehrich, B. Hasse, M. Mausbach, K.G. Müller, IEEE Trans. Plasma Sci. 18 (1990) 895903.
[7] H. Ehrich, B. Hasse, M. Mausbach, K.G. Muller, J. Vac. Sci. Technol. A 8 (1990) 2160–2164.
[8] M.K. Sinha, S.K. Mukherjee, B. Pathak, R.K. Paul, P.K. Barhai, Thin Solid Films 515 (2006) 1753–1757.
[9] M. Mausbach, H. Ehrich, K.G. Muller, J. Vac. Sci. Technol. B 11 (1993) 1909–1915.
[10] H. Ehrich, B. Hasse, K.G. Muller, R. Schmidt, J. Vac. Sci. Technol. A 6 (1988) 2499–2503.
[11] S.K. Mukherjee, M.K. Sinha, B. Pathak, S.K. Rout, P.K. Barhai, A.K. Balamurugan, A.K. Tyagi, F.L. Ng, Thin Solid Films 518 (2010) 5839–5854.
[12] C.B. Boss, K.J. Fredeen, Concepts, Instrumentation and Techniques in Inductively Coupled Plasma Optical Emission Spectrometry, 3rd edition, PerkinElmer, USA, 2004.
[13] J.C.J. Silva, N. Baccan, J.A. Nobrega, J. Braz. Chem. Soc. 14 (2003) 310–315.
[14] A. Sapkota, M. Krachler, C. Scholz, A.K. Cheburkin, W. Shotyka, Anal. Chem. Acta 540 (2005) 247–256.
[15] F.V. Silva, L.C. Trevizan, C.S. Silva, A.R. Nogueira, J.A. Nobrega, Spectrochim. Acta B 57 (2002) 1905–1913.
[16] I.S. Grigoriev, E.Z. Meilikhov, Handbook of Physical Quantities, CRC Press Inc., Boca Raton, 1997.
[17] L. Holland, Vacuum Deposition of Thin Films, Chapman & Hall Ltd., London, 1956.
[18] R. Kaltofen, G. Weise, Surf. Coat. Technol. 74–75 (1995) 469–473.